Energy 317 (2025) 134622

Contents lists available at ScienceDirect

Energy

journal homepage: www.elsevier.com/locate/energy

Large-scale quantification of the future self-covered heat demand using a nationwide residential building database

Katharina Rieck [a,b,*], Kristina Dabrock [a,b], Noah Pflugradt [a], Jann Michael Weinand [a], Detlef Stolten [a,b]

[a] Institute of Energy and Climate Research, Jülich Systems Analysis (ICE-2), Forschungszentrum Jülich GmbH, Wilhelm-Johnen-Str., Jülich, 52428, Germany
[b] RWTH Aachen University, Chair for Fuel Cells, Faculty of Mechanical Engineering, 52062 Aachen, Germany

ARTICLE INFO

Keywords:
Building simulation
Heat demand
Heat pump
Rooftop PV
Self-sufficiency
Germany

ABSTRACT

Electrifying residential heat supply with rooftop photovoltaics (PV) and air-source heat pumps is essential for decarbonizing the German building stock. The potential of these technologies depends on factors such as building properties, rooftop area, weather, and resident behavior. Using a building database and statistical data, we analyzed how much of the residential heat demand in Germany could be independently met by homeowners using PV, heat pumps, batteries, and thermal energy storage. Our energy system model, based on detailed bottom-up building simulations, indicates that 35.2 % of the average annual heat demand can be covered by on-site supply. Grid savings are most significant in well-refurbished single-family and terraced houses, reaching 35 % annually. During cold periods, these houses achieve grid savings of 52%–70%, while in warm periods, they feed 155%–317% surplus electricity back into the grid. Understanding the electricity consumption and grid contributions of solar-assisted heat pumps is critical for accurate grid load forecasting and planning local grid expansions. This knowledge also supports homeowners and policymakers in evaluating the advantages and limitations of these systems, informing subsidy programs and regional energy strategies.

1. Introduction

Residential buildings accounted for 27% of the final energy consumption and 11% of the total greenhouse gas emissions in the European Union in 2021 [1,2]. The biggest share of the residential consumption results from space heating. In Germany, for instance, 65.9% of the residential energy consumption was used for space heating, followed by household uses (lighting, electrical appliances, cooking, and other uses, 17.1%), water heating (16.7%), and space cooling (0.2%) [1]. Space heating in Germany still mostly relies on natural gas (50.8%), and the share of renewables, biofuels, and electricity is at 21.2%, clearly below the average compared to other EU countries [1]. Improving buildings' energy efficiencies and electrifying the residential heat demand by using heat pumps are key factors in reducing energy use and GHG emissions in buildings, as emphasized in the European Green Deal, Renovation Wave Initiative, and the EU's recovery plan [3]. The combination of heat pumps with rooftop PV, as well as thermal and electric storage, is a promising energy system for residential buildings, as a high portion of the heat demand can be covered on-site, reducing grid loads and costs as demonstrated both in theoretical and practical studies [4–14]. By 2030, the German government plans to install 6 million heat pumps, and by 2029, the European Solar Rooftop Initiative aims to make rooftop PV on new residential buildings mandatory [15,16].

The factors influencing electricity consumption and thus the efficiency of the energy system are diverse and depend on various elements such as building properties, rooftop properties, sizing, operating mode and control, residents' behavior, heat distribution, and weather [4,15,17].

The questions we address as part of this study are: (a) how much of the German residential heat demand could be covered on-site if each building used its full rooftop PV potential, considering realistic conditions of the building stock and different influencing factors, and (b) how do heat pump systems combined with rooftop PV impact German grid loads.

Most of the studies in the literature use building simulation tools such as TRNSYS, Modelica, or energy system optimization models [4–11,17–23]. Some of these studies investigate residential energy performance for larger building datasets, considering variations in building

* Corresponding author at: Institute of Energy and Climate Research, Jülich Systems Analysis (ICE-2), Forschungszentrum Jülich GmbH, Wilhelm-Johnen-Str., Jülich, 52428, Germany.

E-mail addresses: k.rieck@fz-juelich.de (K. Rieck), k.dabrock@fz-juelich.de (K. Dabrock), n.pflugradt@fz-juelich.de (N. Pflugradt), j.weinand@fz-juelich.de (J.M. Weinand), d.stolten@fz-juelich.de (D. Stolten).

https://doi.org/10.1016/j.energy.2025.134622
Received 24 July 2024; Received in revised form 14 January 2025; Accepted 17 January 2025
Available online 25 January 2025

properties and occupant behavior [17–23]. For the case of Germany, most of the investigations are conducted for only one or a few individual buildings and they lack a realistic large-scale building stock representation. Literature so far might explain the advantages and feasibility of combined heat pump and PV systems but little is known about the actual energy performance in the German building stock taking real conditions into account. Here, we propose a method to investigate energy load profiles of a building dataset representing the German building stock combined with an energy system model based on a detailed bottom-up building simulation tool (ETHOS.HiSim, [24]). Our scenario analysis depicts flexible processes and dynamic interactions between the different energy system and building components for each house with a high level of detail to approach real conditions and system behavior.

We evaluate the total electricity consumption and see how much the power grid dependency can be decreased by making each building use 100% of their rooftop PV potential. We investigate how much of the heat demand can be covered on-site and what factors have the highest impact on overall energy efficiency. In Section 2, we provide insights into the developed and used methods. In Section 3, we show our key results, which are then discussed and summarized in Sections 4 and 5.

2. Methods

In this study, we aim to investigate how much of the German residential heat demand can be covered on-site by using combined heat pump and rooftop PV systems. For this purpose, we develop an energy demand analysis of a representative German building stock based on a building database and statistical data. For space and water heating, the houses use air–water heat pumps and thermal energy storages (TES).[1] We investigate the overall energy demand and grid dependencies by comparing two scenarios: scenario (a) where zero PV is used and electricity demand for heating and household appliances is covered 100% from the grid versus scenario (b) where each building uses its full rooftop PV potential in combination with a battery storage and an energy management system for optimal self-consumption. With the building simulation tool ETHOS.HiSim [24], we generate an energy system model and simulate energy load profiles for each building in a 1-year simulation of 1-min time resolution.

2.1. Generation of household and building dataset

The German building stock contains 19.5 million residential buildings [25]. As we cannot simulate such a high number of buildings (the simulation of one house takes 4 min and with our resources only 100 houses can be calculated in parallel), we generate a representative distribution of the German building stock based on 10,000 different building and 22,176 household configurations. These configurations are used later for the ETHOS.HiSim simulation. The residential buildings are taken from the building database ETHOS.BUILDA v.1.0.0 [26] containing information about Tabula building code describing building type, construction year class and refurbishment state, the heated floor area, norm heating load, postal code, and the rooftop PV capacity. Subsequently, we randomly assign the rooftop PV tilt and azimuth values based on data from Risch et al. [27], and distribute households based on statistical data from the census [28]. These samples are referred to as our building dataset.

[1] TES: thermal energy storage.

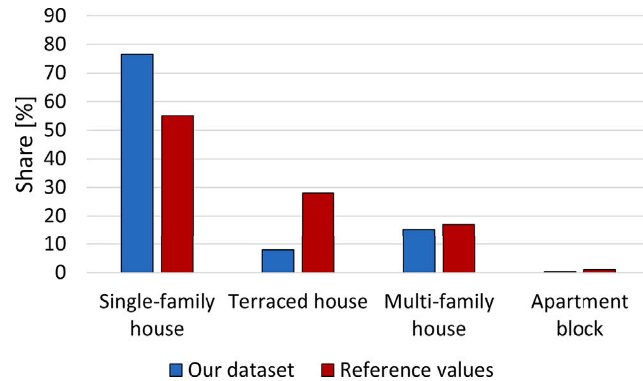

Fig. 2.1. Shares of building types in our building dataset compared to Tabula reference values.

2.1.1. German residential building properties

As described in Dabrock et al. [29], the foundation of building data in ETHOS.BUILDA comes from official 3-D building datasets and OpenStreetMap data. These datasets provide basic information on the location and footprint of buildings. Some additional information, e.g., on the usage type of a building and the height, is available in the 3-D building data, and occasionally also in the OpenStreetMap data. In ETHOS.BUILDA, the basic building data is enriched with additional datasets, and machine learning is applied to impute missing data.

Building codes

One of the most important building attributes for this study is the Tabula type which provides standardized information about energy-related parameters and building construction data [30]. Studies have used and validated this model and confirmed it as useful instrument to assess the energy performance of existing building stocks [31–34]. Still, the accuracy of this model depends much on the availability of statistical building stock data and on how Tabula building codes are assigned to individual buildings [34,35]. In this study ETHOS.BUILDA assigns the Tabula type based on a separate assignment of size class, construction year, and refurbishment states, which then allows the derivation of Tabula building codes [29]. As none of the three attributes is available on a building level, ETHOS.BUILDA used a machine learning approach. Labeling of training samples was based primarily on the German census of 2011 [28], and a range of building and neighborhood morphological characteristics combined with socioeconomic data served as features for training a machine learning model. As discussed in Dabrock et al. [29], a slight overrepresentation of the majority classes of both size class and construction year can be observed. For size classes, this is apparent in the comparison between our dataset and the Tabula reference values (see Fig. 2.1), which shows that our dataset contains 22% more single-family houses (SFH)[2] and 20% fewer terraced houses (TH)[3] than the reference data from the Tabula statistics (see Fig. A.1, [36,37]). The shares of multi-family houses (MFH)[4] and apartment blocks (AB)[5] in our dataset are relatively accurate with only 2% and 0.7% deviation from the reference values.

Similarly, common construction year classes such as generation 04, 05 and 06, as represented in Fig. A.1, occur more frequently, leading to a larger number of SFHs of these generations in our dataset than in the reference dataset. Deviations in the shares of the construction year classes are expected not to have a high impact on the energy performance, though, as the energy consumption depends more on individual conditions such as energy system and efficiency [29,38].

[2] SFH: single-family house.
[3] TH: terraced house.
[4] MFH: multi-family house.
[5] AB: apartment block.

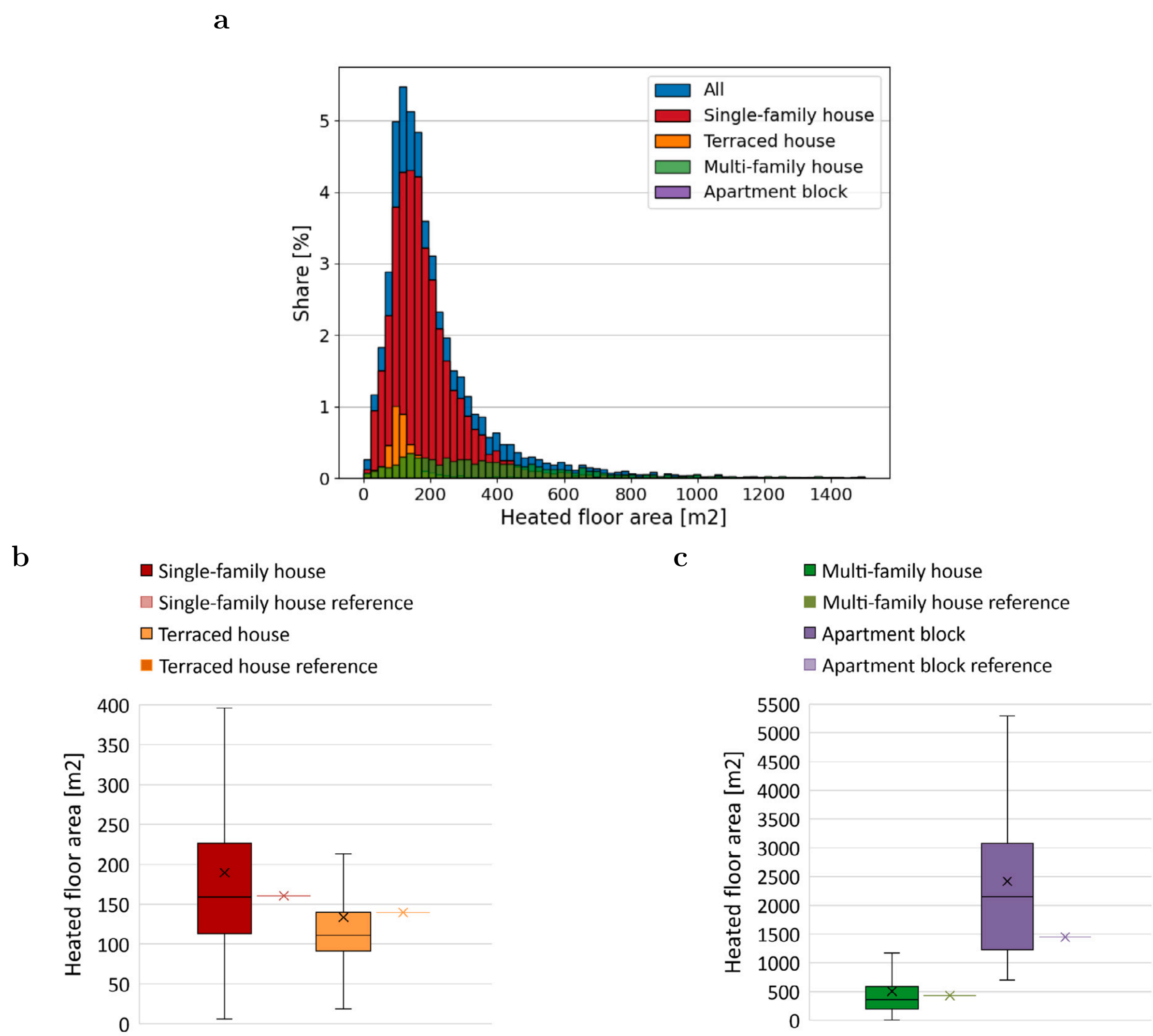

Fig. 2.2. Heated floor area [m^2] in our building dataset. (a) Distribution of heated floor areas [m^2] in our building dataset sorted according to building types. (b) heated floor area [m^2] compared to the Tabula reference mean values [37] for SFH and TH. (c) heated floor area [m^2] compared to the Tabula reference mean values for MFH and AB. The x represents the mean value. Outliers are removed.

Heated floor area

The calculation of the conditioned living area in ETHOS.BUILDA is described in Dabrock et al. [29]. The distribution of the heated floor areas (see Fig. 2.2a) in our dataset shows that the range of MFHs is much wider and extends to higher areas than that of SFHs and THs. This is expected, as SFHs and THs are buildings with 1–2 apartments and MFHs cover a much wider range of 3–12 apartments. ABs are hardly visible in this figure as their share is only 0.3% in the building stock. As shown in Fig. 2.2b and c, there is a high agreement between our dataset and the reference dataset for THs and MFHs. The average heated floor areas for THs and MFHs in our dataset are 134 m^2 and 504 m^2, respectively. The reference areas for these types are 140 m^2 and 430 m^2. For SFHs and ABs, our average heated floor areas (190 m^2 and 2419 m^2) are higher than the reference areas (161 m^2 for SFH and 1445 m^2 for AB). This might be due to the observation that the OpenStreetMap input data occasionally contains building entries that in reality are likely multiple buildings, e.g., a block of ABs or a row of THs mistakenly recorded as one large building.

2.1.2. Rooftop PV capacity potential and orientation

In this study, we only investigate rooftop PV for residential buildings. Facade PV is neglected due to its higher costs and lower efficiency [39–42]. External solar farms are not taken into account and solar energy is produced on-site to avoid the need of transportation and the strain on electricity grid capacity. Rooftop PV capacities were assigned to all buildings in ETHOS.BUILDA by spatially joining the per-roof results from Risch et al. [27] with the building footprint polygons and summing up the capacity values to derive one capacity value per building. The distribution of capacities in our dataset is shown in Fig. 2.3a. The average rooftop PV capacity is 15.5 kW.

The distributions for the rooftop azimuth and tilt angles are aligned with the rooftop PV potential data from Risch et al. [27] (see Fig. 2.3b and c). The rooftop azimuth angles are distributed symmetrically with the highest counts in the South and North directions, followed by East and West directions (see Fig. 2.3b). The mean azimuth angle is 183° (South). The rooftop tilt angles are limited between 10° and 90°. According to Risch et al. [27], roofs with tilt angles lower than 10° were assumed to be flat. Risch states that PV modules on flat roofs were placed at an optimal tilt angle in the South direction, similar to Ryberg's work [43]. Here, the most represented roof tilt angles are 45° and 10° (see Fig. 2.3c). In our dataset, lower tilt angles (<20°) are slightly overrepresented and higher angles (>40°) are slightly underrepresented compared to the reference values from Risch et al. The German mean tilt angle is 32°, which is very close to the mean tilt value of 31.6° found in Killinger et al. [44]. Two shares of maximum PV rooftop potential (0% for no PV use and 100% for use of full PV potential) are evaluated.

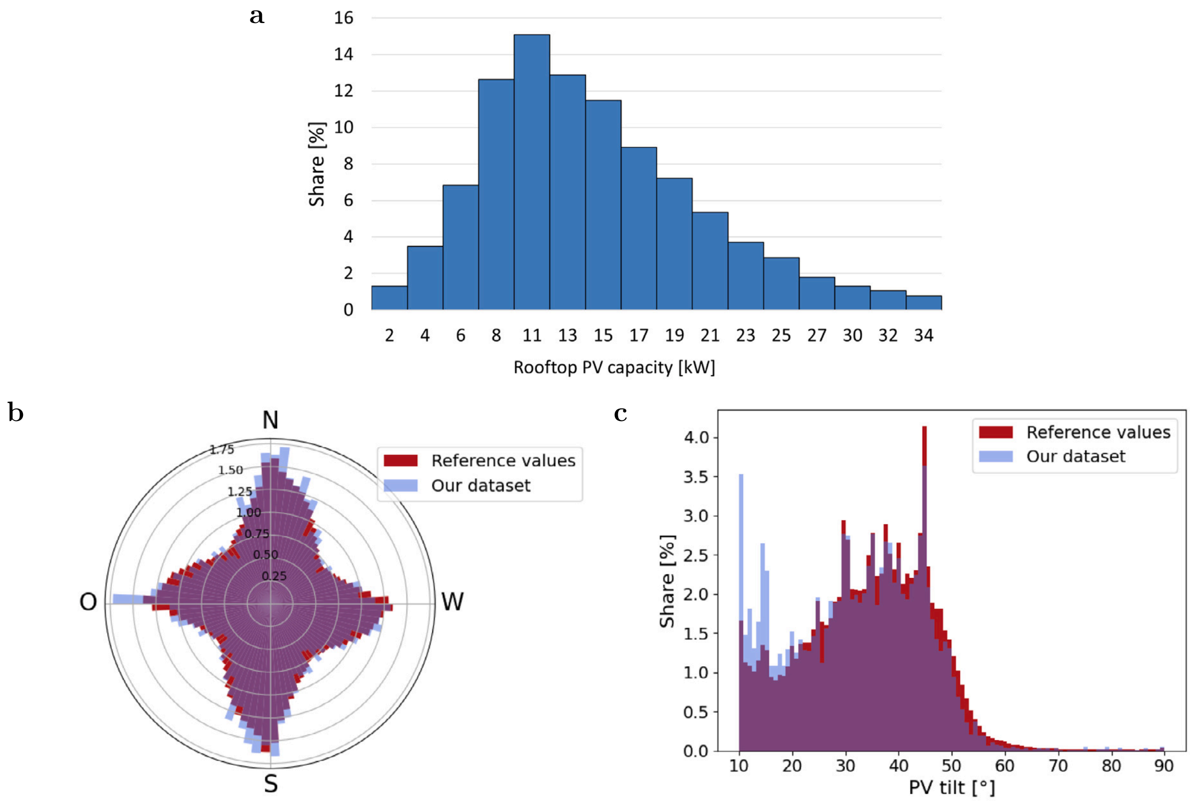

Fig. 2.3. Rooftop PV data in our building dataset. Reference values are the results of Risch et al. [27]. (a) Shares of rooftop PV capacities in our building dataset. Outliers are removed. (b) Shares of rooftop PV azimuth angles in our building dataset. Radii represent shares in %. (c) Shares of rooftop PV tilt angles in our building dataset.

2.1.3. Building location, weather profiles and norm heating load

Buildings in ETHOS.BUILDA were assigned postal codes by spatially joining a postcode dataset for Germany based on the position of the building's centroid [45]. In Fig. 2.4a, the spatial distribution of our building dataset is shown, sorted according to the four building types SFH, TH, MFH and AB. We can see that SFHs are the most represented and are distributed all over Germany in urban and rural areas. In densely populated areas, such as the western part of Germany or cities such as Hamburg and Berlin, the ratio of other building types such as TH, MFH, and AB is high compared to rural areas. ABs are especially often represented in Berlin.

Each postal code is assigned a Test Reference Year (TRY)[6] region with the climate data of the DIN norm DIN/TS 12831-1 [46]. Fig. 2.4b shows the spatial distribution of our building stock according to the 15 different TRY regions (see also Table A.2 and Fig. A.2). The TRY region 11 (Fichtelberg) is the region with the coldest climate, and region 12 (Mannheim) is the region with the warmest climate (see Fig. 2.4c). Depending on the climate, location height, and thermal building properties, the norm heating load of each building is calculated and used for scaling the energy system in order to meet the individual heating demands. According to the DIN norm DIN/TS 12831-1 [46], the heating reference temperature of each building location takes into account the location height and time constant. The final norm heating load in Watts is obtained as:

$$\Phi_{norm} = (H_{trans} + H_{venti}) * (T_{initial} - T_{ref}) \quad (1)$$

where H_{trans} and H_{venti} are the heat transfer coefficients for transmission and ventilation in Watts per Kelvin, $T_{initial}$ is the initial temperature of the building, and T_{ref} is the heating reference temperature. For our building dataset, we get the following norm heating loads (see Fig. 2.5).

The norm heating load of the average building is 11 kW. ABs have the highest heating loads and THs have the lowest.

2.1.4. Households and resident behavior

The energy demand of a building depends on the resident behavior and household load profiles [17,18,23,47]. With the help of the LoadProfileGenerator (LPG,[7] [48]), 64 different household types can be generated with varying numbers of residents and various lifestyles and routines. Each household offers specific load profiles such as water, heat, and electricity demand, as well as internal heat gains such as heating by residents and heating by devices.

To represent the German households, a Monte Carlo distribution is made based on census data of German household types, number of persons, and working status [28]. Based on these household types, the corresponding LPG household models are chosen for each dwelling in the building. When the same profile exists more than once in a building, a unique identifier is used to slightly vary the occupant load profiles, ensuring they diverge from each other. Fig. 2.6a and b show the different household types and number of residents in our dataset compared to the reference data from the census [28]. Our values are very similar to the input data from the census with less than 1% deviation.

The energy consumption in our residential building stock is also related to the residents' behavior. This is why working status information from the census is taken into account [28]. Fig. 2.6c shows the shares of working residents per household in the building dataset. In most households, all residents are unemployed (working status is 0%). This category includes jobless persons, children, and seniors. Twenty-seven percent of the households have a full working status (working status is 100%). On average, the working status of our household is 46%. This

[6] TRY: Test Reference Year.

[7] LPG: LoadProfileGenerator.

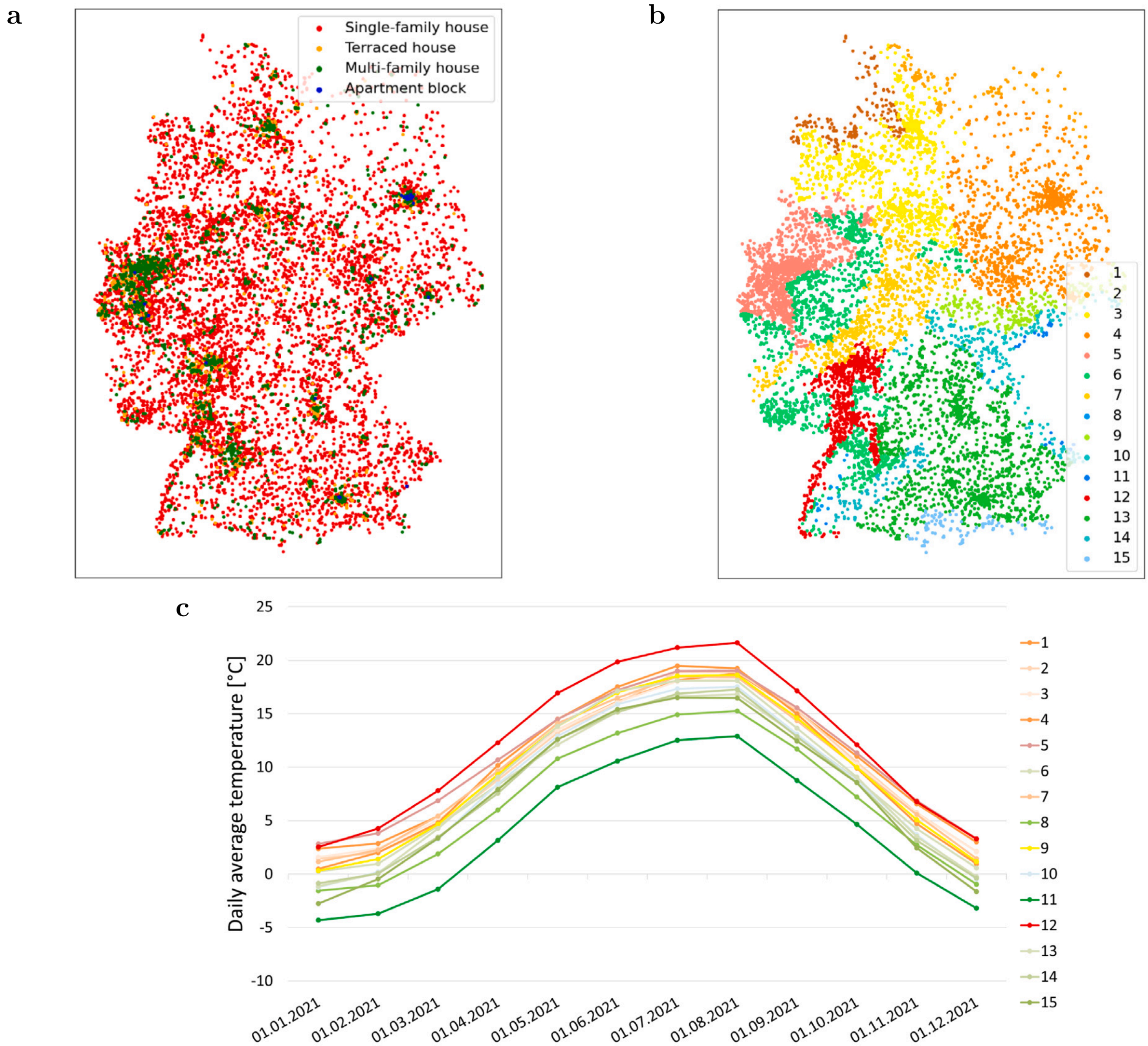

Fig. 2.4. Building locations in our building dataset sorted according to building types and TRY weather regions. (a) Building locations of our building dataset sorted according to building types. (b) Building locations of our building dataset sorted according to TRY weather regions. (c) Daily average temperatures [°C] for all 15 TRY regions in our building dataset.

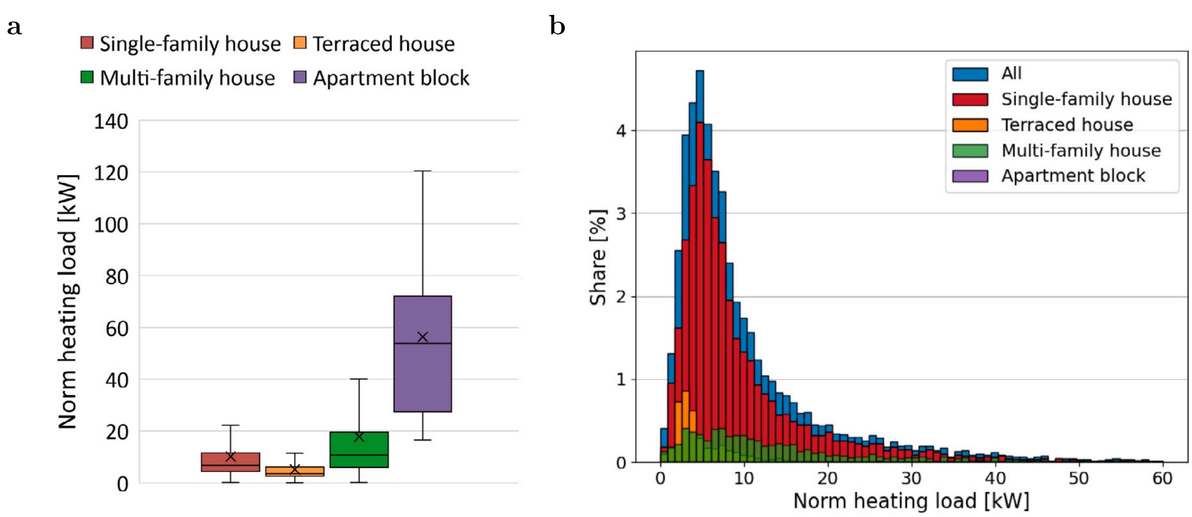

Fig. 2.5. Norm heating loads [kW] in our building dataset sorted according to building types. (a) Norm heating loads for each building type. Outliers were removed. The *x* represents the mean value. (b) Norm heating load distributions of each building type and shares [%] in our building dataset.

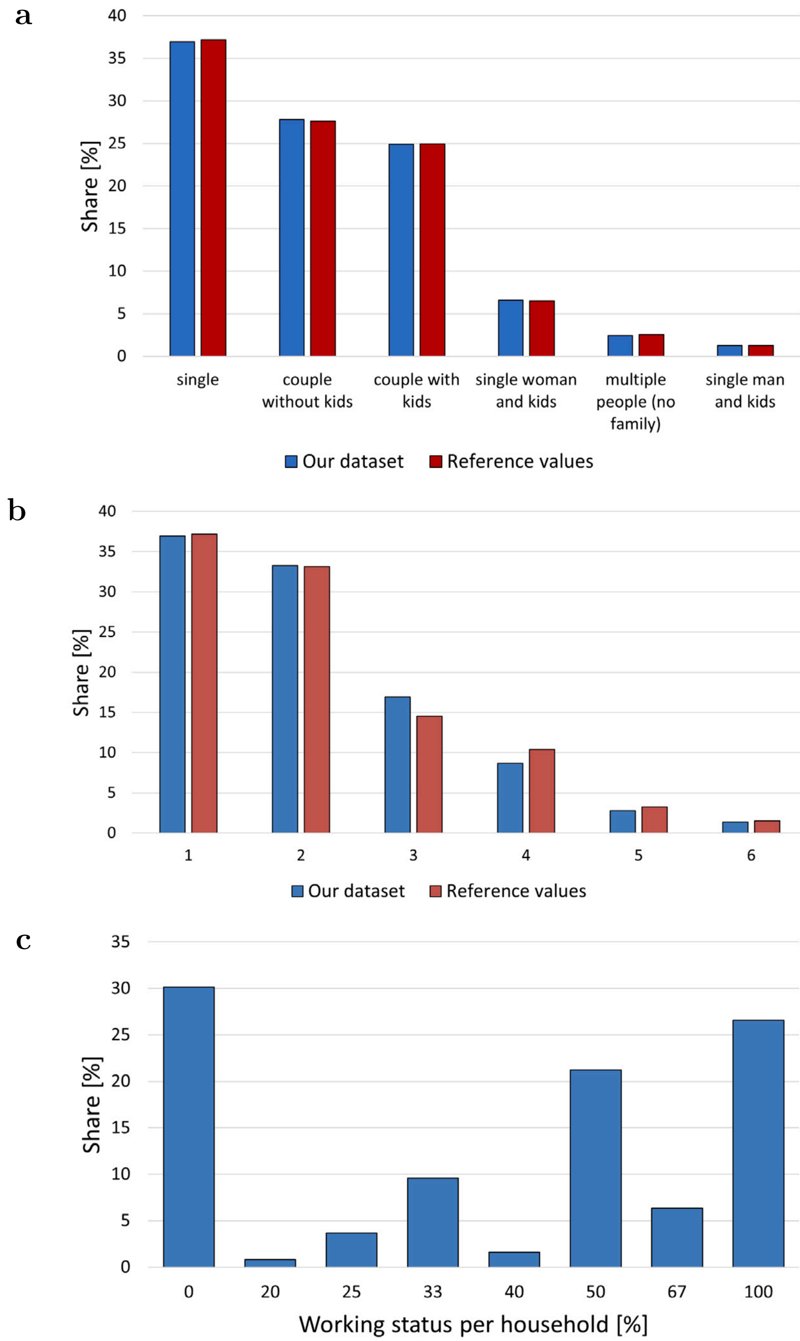

Fig. 2.6. Household types and residents in our dataset. (a) Share of household types in our building dataset compared to reference values from census [28]. (b) Share of number of residents per household in our building dataset compared to reference values from census [28]. (c) Share of working residents per household in our building dataset. 0% = no person in this household has a job. 100% = all persons in this household have a job.

is slightly less than the census reference data [28], where 51.5% of the German population is employed.

2.2. Building and load profile simulation with ETHOS.HiSim

Each of the buildings and households in our building dataset is simulated and analyzed with a bottom-up model called ETHOS.HiSim [24].

ETHOS.HiSim is a modular, open-source simulation tool that allows dynamic all-year time step simulations of building and energy system components with closed control loops. Similar to TRYNSYS it enables circular dependencies between the different system components by doing iterations inside each time step. Different households can be constructed, including the building envelope, household with residents, weather profiles, and various energy system combinations. The time resolution is chosen to be one minute.

2.2.1. Building infrastructure model

Here we want to investigate how much of the annual heat demand can be covered independently from the electricity grid in German buildings. Therefore, we created a housing model based on an air–water heat pump system combined with TES and investigated the effect of adding rooftop PV (plus battery storage and energy management) on grid consumption and self-sufficiency rates (see Fig. 2.7).

For space heating and domestic hot water the model uses two separate air–water heat pumps in combination with a TES. The heat pump model in ETHOS.HiSim is based on the python package hplib [49]. It

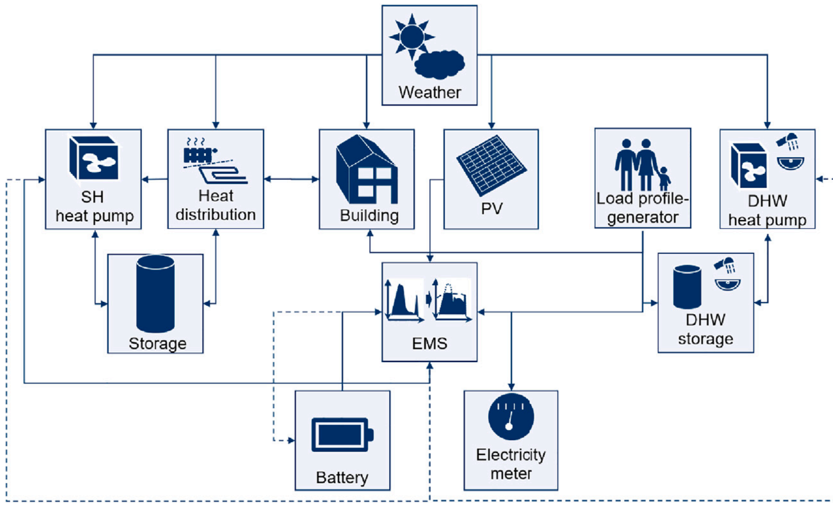

Fig. 2.7. House with air–water heat pump, thermal energy storage, PV system, battery storage and energy management system. SH = space heating, DHW = domestic hot water.

is an open-source simulation tool that identifies efficiency parameters from a real heat pump measurement database with a least-square regression model and generates time series of heat pump efficiency (COP), thermal and electrical power and mass flow. The method is based on Schwamberger [50] and the MATLAB-toolbox CARNOT [51, 52]. As the heat distribution system, we choose floor heating, which allows better heat pump performance [53,54]. The heat distribution system calculates daily set flow temperatures based on a heating curve and simulates the heat exchange between the building and the hot water. To reduce electricity consumption from the grid, a rooftop PV system is used in combination with battery storage and an energy management system. The PV system model is based on a python package pvlib [55–57] which simulates electrical power with respect to the PV system parameters and the weather input data. The battery storage originates from a model called bslib [58] which simulates electrical power and state of charge. If the rooftop PV electricity production exceeds the total electricity demand of residents, electrical devices, and heat pumps, the battery storage is charged. If the battery is charged to 100% and surplus electricity is still available, the set temperatures for the TES are increased by 10 °C, and the set heating temperature of the building indoor air is increased by 2 °C. In this way, surplus electricity can be stored as thermal energy in the water tanks and the house for flexible use.

The building envelope is modeled based on the RC simulator [59], which uses the norm DIN EN 13790 [60] and building property data from Tabula [61], including thermal resistances and heat transfer coefficients based on the building code given by the configuration. Heat losses result from transmissions and ventilation, while heat gains come from solar gains through windows and internal gains from residents and electrical devices. Taking into account these parameters and the difference between the indoor air and set temperature (20 °C), the current heating demand is calculated according to ISO 13790.

An electricity meter tracks electricity consumption and production, calculating how much is taken from or fed into the electricity grid.

Given that residential cooling accounts for less than 1% of European residential energy consumption [1], space cooling is not considered in this study.

2.2.2. Energy system sizing

Each energy system component has its size and capacity adapted to the building properties to ensure that energy demands can be fulfilled. The sizes of the aforementioned components are based on the maximum thermal load of the building and the size and number of apartments (see Table 1).

Table 1
Energy system sizing. TES — thermal energy storage, SH — space heating, DHW — domestic hot water.

Energy system	Sizing	
component	Variable	Equation
Heat pump (SH)	Thermal power	Eq. (2)
TES (SH)	Volume	Eq. (3)
Heat pump (DHW)	Power	Eq. (4)
TES (DHW)	Volume	Eq. (5)

The heat pump power is chosen equal to the heating load:

$$P_{HP^{thermal}} = \Phi_{norm} \tag{2}$$

The TES sizes are also adapted accordingly:

$$V_{buffer} = \frac{\Phi_{norm} \cdot T_{bridge}}{c_w \cdot (T_{flow^{max}} - T_{return^{max}})} \tag{3}$$

where Φ_{norm} denotes the heating load of the building, T_{bridge} is the bridging time of 1 h, c_w is the specific heat capacity of water, $T_{flow^{max}}$ is the maximum flow temperature of the heat distribution system, and $T_{return^{max}}$ is the maximum return temperature [62].

To achieve an optimal self-sufficiency rate, it is suggested to install 1 kWh of battery capacity per 1 kWp of rooftop PV power [63].

The domestic hot water heat pump and storage system are scaled up with the number of apartments in the building:

$$P_{HP^{DHW}} = 300\ \mathrm{W} \cdot N_{DB} \tag{4}$$

$$V_{DHW} = 230\ \mathrm{l} \cdot N_{DB} \tag{5}$$

2.2.3. Validation of heating demand

The average heating demand for space heating and domestic hot water in the presented model is 21.6 MWh and 6.2 MWh, respectively, resulting in a total heating demand of 27.8 MWh per building per year. This theoretical absolute value closely aligns with the reference value reported by the German DENA building statistics in 2024, which cites an average heating demand of 27.4 MWh per residential building per year for space and domestic hot water heating [64]. To validate the time series data of our model, the daily average heating demand per building was evaluated as a function of the daily average outside temperature (see Fig. 2.8). The theoretical heating demand was successfully fitted using a Sigmoid function, commonly applied in modeling and forecasting residential gas demands [65–68].

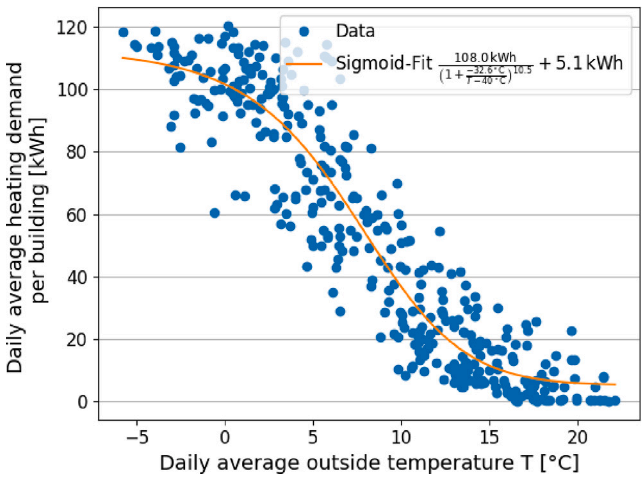

Fig. 2.8. Validation of the daily average heating demand per building. The modeled data is fitted with a Sigmoid function which is commonly used in modeling and forecasting residential gas demands in relation to the daily average outside temperature T [65–68]. The Sigmoid-Fit was generated based on a non-linear least squares method.

3. Results

The results encompass electricity consumption, grid dependencies, and self-sufficiency rates, with a focus on self-covered heat demand distributed over one year for German buildings utilizing different shares of rooftop PV potential.

3.1. Impact of rooftop PV on grid consumption

Without the use of PV, the total annual electricity consumption of an average building in our dataset is 14.9 MWh (see Fig. 3.1a and Table A.1). The mean grid consumption for space heating is 5.0 MWh, which accounts for 33% of the total consumption (see Fig. 3.1b). When utilizing the full rooftop PV potential for each building, combined with a battery storage, thermal energy storage and an energy management system, the mean annual grid consumption of the dataset decreases by 42.9% to 8.5 MWh. The grid consumption for space heating decreases by 35.2% to 3.2 MWh per building.

Fig. 3.1c shows the rooftop PV production per building, sorted according to different building types. On average, full rooftop PV systems produce 13.5 MWh of electricity per building per year. As SFHs are the most prevalent building type, their average annual rooftop PV production is close to the total average at 13 MWh, with a mean PV rooftop capacity of 15 kW. THs, having relatively smaller rooftop areas and PV capacities, supply on average 8.2 MWh of PV electricity. MFHs, with larger rooftop areas, result in an average PV generation of 17.8 MWh. Although ABs constitute only 0.3% of the building stock, their rooftop PV generation is surprisingly high at 39 MWh per average building, owing to their very large rooftop areas ($\Omega = 554$ m^2) and PV capacities ($\Omega = 42$ kW).

On average, 36% of the PV electricity is used directly on-site for household needs and electrical devices (residents), space heating (SH heat pump), and domestic hot water (DHW heat pump) (see Fig. 3.2a and Table A.1). When surplus PV electricity is available, 18% is used for charging the battery storage. If the battery storage is full, the energy management system increases the set temperatures of the water storage tanks and the building's indoor air to store surplus electricity as thermal energy. Through this load-shifting approach, grid consumption can be reduced by 3% and grid injection by 6% (see Fig. A.3). If excess electricity still remains after load shifting, 46% of the solar energy is fed into the grid. When PV production is insufficient to meet electricity demand, the remaining energy is drawn from the grid (see Fig. 3.2b). The average self-sufficiency rate of the total building stock is 52.9%, representing the percentage of energy demand met through on-site generation. Grid consumption for different electricity consumers decreases by 40.6% for residents, 35.2% for the SH heat pump, and 83.5% for the DHW heat pump, respectively. On average, residents account for 55%, the SH heat pump for 32%, the DHW heat pump for 9%, and battery losses for 4% of the total electricity consumption.

3.2. Grid consumption for different building types

The amount of electricity each building requires for heating and household purposes depends strongly on building properties, such as building type and size. Fig. 3.3a and b show grid consumption for different building types when no rooftop PV is used.

As ABs represent the largest building types (see Fig. 2.2), they have the highest mean electricity consumption at 141 MWh. They are followed by MFHs with 35 MWh, SFHs with 11 MWh, and THs with 9 MWh (see Fig. 3.3a).

For space heating, the trend is similar (see Fig. 3.3b). ABs have the highest electricity consumption for space heating (Ø= 18.9 MWh), followed by MFHs with 7 MWh, SFHs with 4.8 MWh, and THs with 2.1 MWh. Depending on the ratio between PV production and electricity consumption, different self-sufficiency rates can be observed for individual building types. Self-sufficiency is highest for SFHs (Ø= 55%), followed by THs (Ø= 53%), then MFHs (Ø= 41%), and lowest for ABs (Ø= 29%) (see Fig. 3.3c). For space heating, this trend is slightly different. Here, THs have the highest self-sufficiency rates (Ø= 35.3%) because their space heating consumption is the lowest (see Fig. 3.3d). The correlation between conditioned floor area and the self-sufficiency rate for space heating (see Fig. 3.4a) shows that self-sufficiency decreases with increasing floor area. For small floor areas, the decline is steep, whereas for larger floor areas, the self-sufficiency rate decreases more gradually. We choose a logarithmic function for the regression. For apartment blocks, the sample size is too small to perform a regression analysis, but we estimate a similar behavior. According to the fit function, the constant term and the absolute value of the coefficient are highest for THs and lowest for MFHs. This behavior can be explained by the fact that the self-sufficiency rate for space heating depends on the ratio between PV production and space heating demand. For small THs, the electricity demand is sufficiently low to achieve high self-sufficiency rates, whereas for larger THs, rooftop PV potentials do not increase as much and cannot fully compensate for consumption. For very small conditioned floor areas (<50 m^2), space heating demands tend to be very low, and self-sufficiency rates very high, because other heating effects, such as heating from residents and electrical devices, play a larger role and reduce the overall electricity consumption.

Fig. 3.4b shows the self-sufficiency rate of space heating for different building types and construction year classes (see Fig. A.1). SFHs constructed between 1979 and 1983 [construction year class 07] exhibit the highest self-sufficiency rate for space heating (Ø= 40.5%), followed by SFHs constructed between 2002 and 2009 [construction year class 10] with a mean space heating self-sufficiency of 39.9%. The lowest space heating self-sufficiency rate is observed for ABs, particularly for ABs from the construction year class 05. A general correlation between building age and energy consumption could not be observed, as individual conditions such as energy efficiency and energy systems determine the consumption [38].

3.3. Daily impact on grid

Decarbonizing the German building stock and transitioning from fossil fuel-based heating systems to solar-assisted heat pumps will significantly impact electricity grid loads, leading to higher peak loads and fluctuations. Stabilizing and adapting electricity grids to these new conditions is a crucial step in the thermal energy transition in

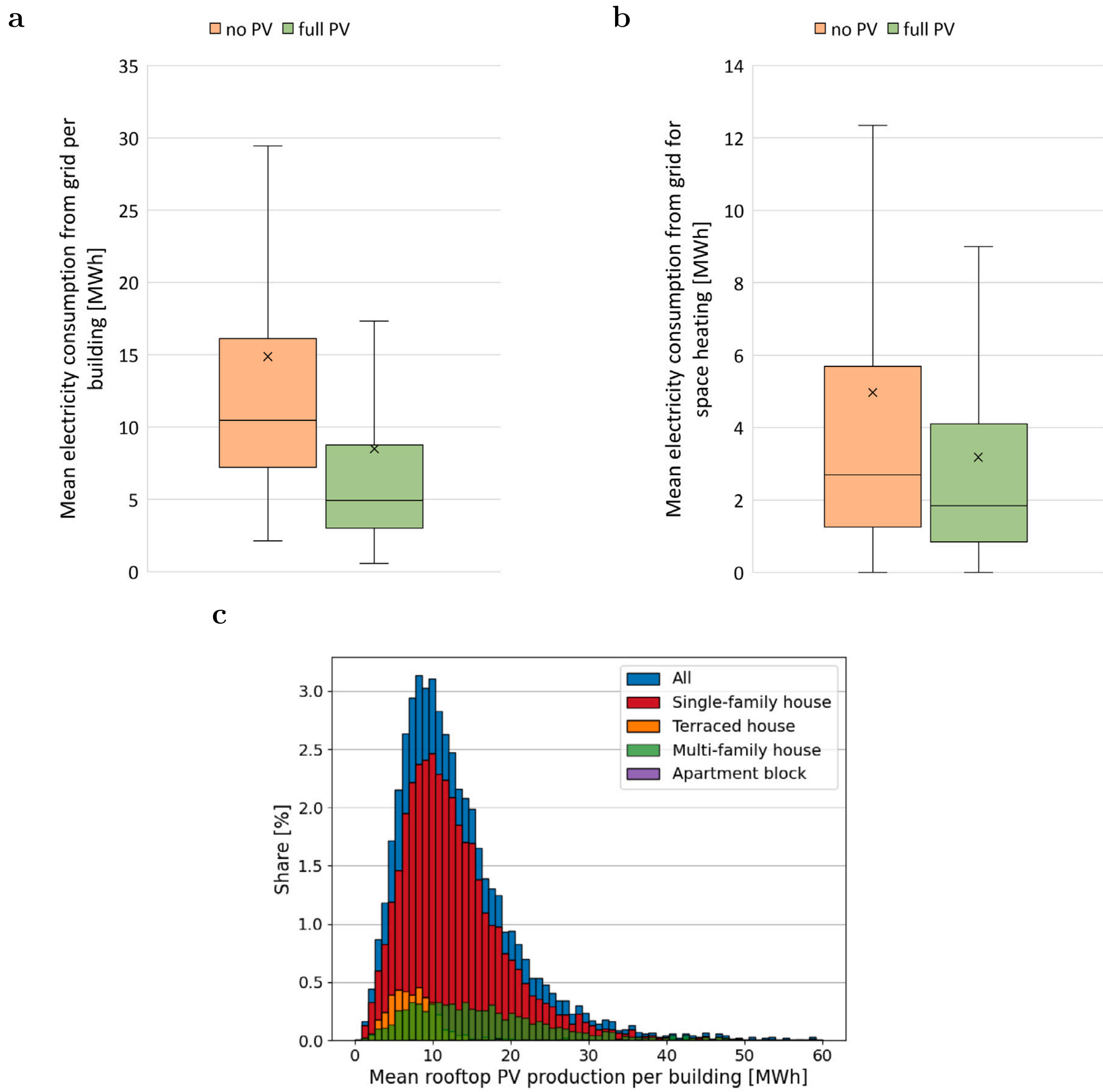

Fig. 3.1. Mean annual grid consumption and rooftop PV production [MWh] per building in our building dataset. (a) Total mean grid consumptions per building [MWh] without and with rooftop PV. Outliers were removed. The *x* represents the mean value. (b) Mean grid consumptions per building [MWh] for space heating without and with rooftop PV. Outliers were removed. The *x* represents the mean value. (c) Mean annual rooftop PV production distributions [MWh] of each building type and shares [%] in the building stock.

Germany. An essential aspect of expanding the power grids is the needs assessment and evaluation of where and how many grids need to be expanded. Our analysis shows how full rooftop PV utilization combined with heat pumps in the German building stock could impact daily grid consumption, considering different building types and ages (see Fig. 3.5a–d). We investigate how much electricity from the grid is saved with 100% rooftop PV compared to 0% PV. Savings exceeding 100% represent grid injections. In general, all buildings with full PV depend less on the grid than without PV. In the summer months (April to September), smaller building types (SFHs and THs) produce more energy than they consume and inject up to 90 kWh per day into the grid. SFHs (Fig. 3.5a) achieve the highest grid savings among the different building types. In cold periods (October to March), they show an average load reduction of 70% when using their full rooftop PV potential. During warmer months, all SFH classes show average grid savings of up to 317%. SFHs constructed before 1859 (DE.N.SFH.01) and between 1979 and 1983 (DE.N.SFH.07) exhibit the highest grid injection in July. The lowest grid consumption in January and December comes from young SFHs built between 2002 and 2009 (DE.N.SFH.10), while the highest consumption results from houses built between 1949 and 1968 (DE.SFH.05 and DE.N.SFH.04). Except for the latter, with rooftop PV, all SFHs consumed less electricity from the grid than the average SFH without PV throughout the year.

The same applies to THs (Fig. 3.5b). Compared to SFHs, they show fewer grid injections between April and September, as their rooftop areas and PV potentials are much smaller. However, THs also have lower grid loads in cold months such as January and December. THs achieve average grid savings of 52% during colder periods (October to March) and 195% during warmer periods (April to September). Their maximum grid injection is 48 kWh per day in July (DE.N.TH.02). Some MFHs (Fig. 3.5c) show higher grid injections than THs, due to their higher rooftop PV potentials. For example, DE.N.MFH.09, constructed between 1995 and 2001, has a maximum grid injection in July of 130 kWh per day. Still, most MFHs do not produce enough PV electricity in the summer months to fully compensate for their consumption. The highest grid consumption in winter for MFHs comes from DE.N.MFH.07, built between 1979 and 1983. Nevertheless, the grid consumption of MFHs using PV is much less compared to without PV. In cold periods (October to March), average grid savings of 26% are achieved, and in warmer periods (April to September), even 97%. Due to their high electricity

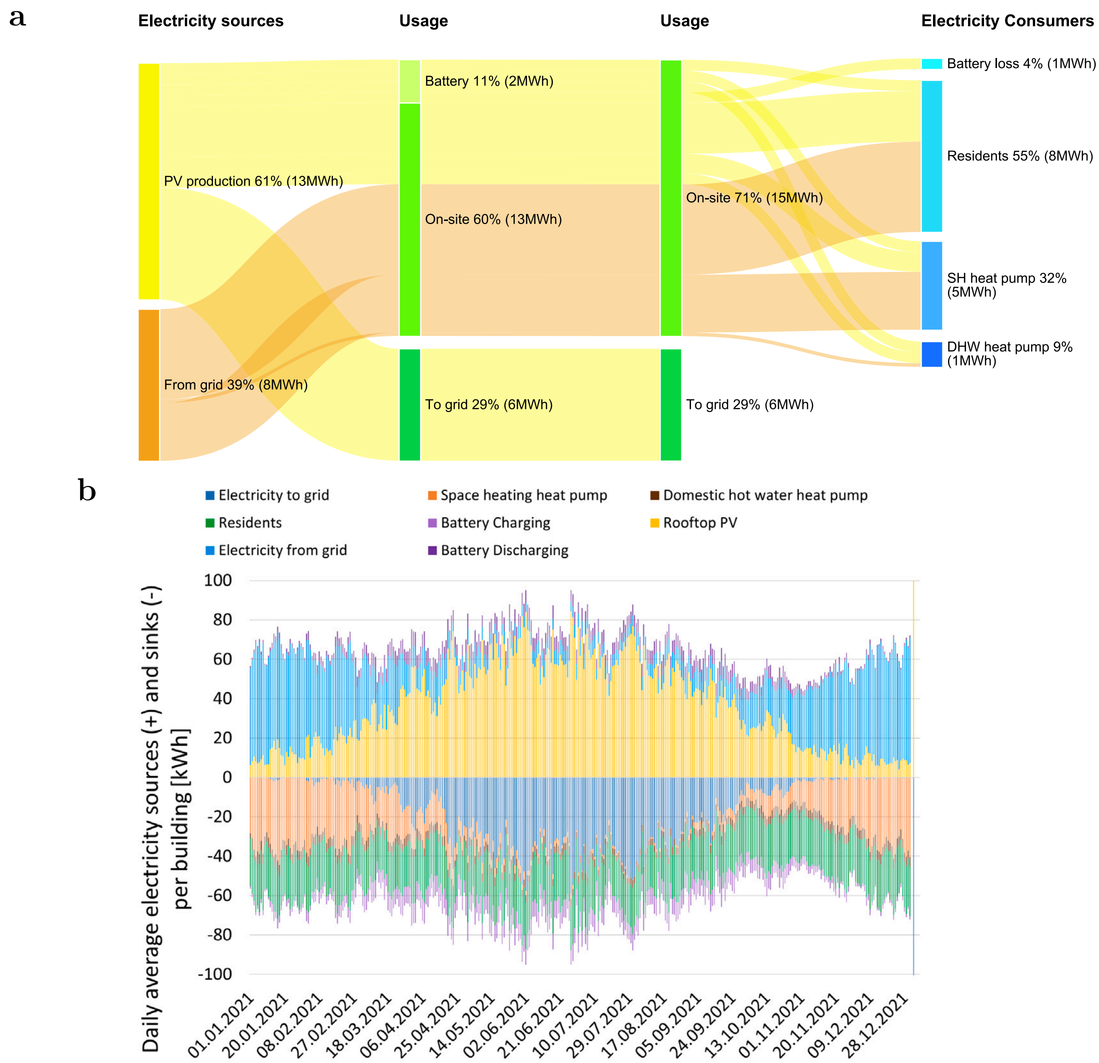

Fig. 3.2. Annual electricity sources and sinks of the building dataset. (a) Flow chart of mean annual electricity production and consumption per building. This chart describes average values. Numbers are rounded up. (b) Daily average electricity sources (+) and sinks (−) per building.

consumption and relatively low rooftop PV production, ABs have the highest grid consumption and do mostly not attain a state of surplus electricity even in summer (Fig. 3.5d). The comparison of ABs with 0% rooftop PV versus 100% rooftop PV reveals that grid loads can be reduced by 14% during colder months (October to March) and by 41% during warmer months (April to September). Most of the electricity is consumed by DE.N.AB.05 houses, which were constructed between 1958 and 1968. The highest grid injection in summer is from DE.N.AB.02 (built between 1860 and 1918), with 11 kWh injection per day resulting in grid savings of 109% compared to the mean reference value without PV.

4. Discussion

The main goal of this study is to quantify how much of the German residential heat demand could be covered on-site using air-source heat pumps combined with rooftop PV and energy management. First, we discuss our results in the context of existing literature: we found grid savings of 46% for space and water heating when using full rooftop PV potential and a flexibility strategy. Similar to the studies of Battaglia et al. [8], Bee et al. [4], and Eicke et al. [69], we observed increased self-sufficiency rates when supporting our solar-assisted heat pumps with thermal and electric storage and an energy management system, as the electricity load for heating could be shifted to times of higher solar gain. The overall grid consumption of our building dataset could be reduced by 42.9 %.

If we multiply the mean grid consumption per year of our building dataset (see Table A.1) by the total number of residential buildings in Germany (19.5 million), the use of solar-assisted heat pumps in German residential buildings would result in an annual grid load of approximately 166 TWh. This is 16% higher than the electricity demand for households in 2021 [70]. Based on our mean annual grid injection of 6.2 MWh, the total annual grid injection for all of Germany would be 121 TWh. This is 56% more than the German grid injection from photovoltaics in 2023 [71]. These results are relevant for the needs assessment of future electricity grids in Germany. SFHs are the most represented residential buildings in Germany, and they show reduced grid loads in cooler periods of the year. In warmer periods, they achieve high surplus energies, even though storage systems and energy management already optimize self-consumption. This means high grid injections are expected in the summer months, further substantiating the necessity of grid expansion in most regions of Germany. We found that space heating and domestic hot water account for 32% and 9% of the overall electricity consumption, respectively; the remainder comes from household electrical devices (55%) and battery losses (4%). This is similar to the proportions shown in Battaglia et al. [8], where the electricity load of a single-family house was 34.8% for space heating, 19.3% for domestic hot water, and 45.9% for household appliances.

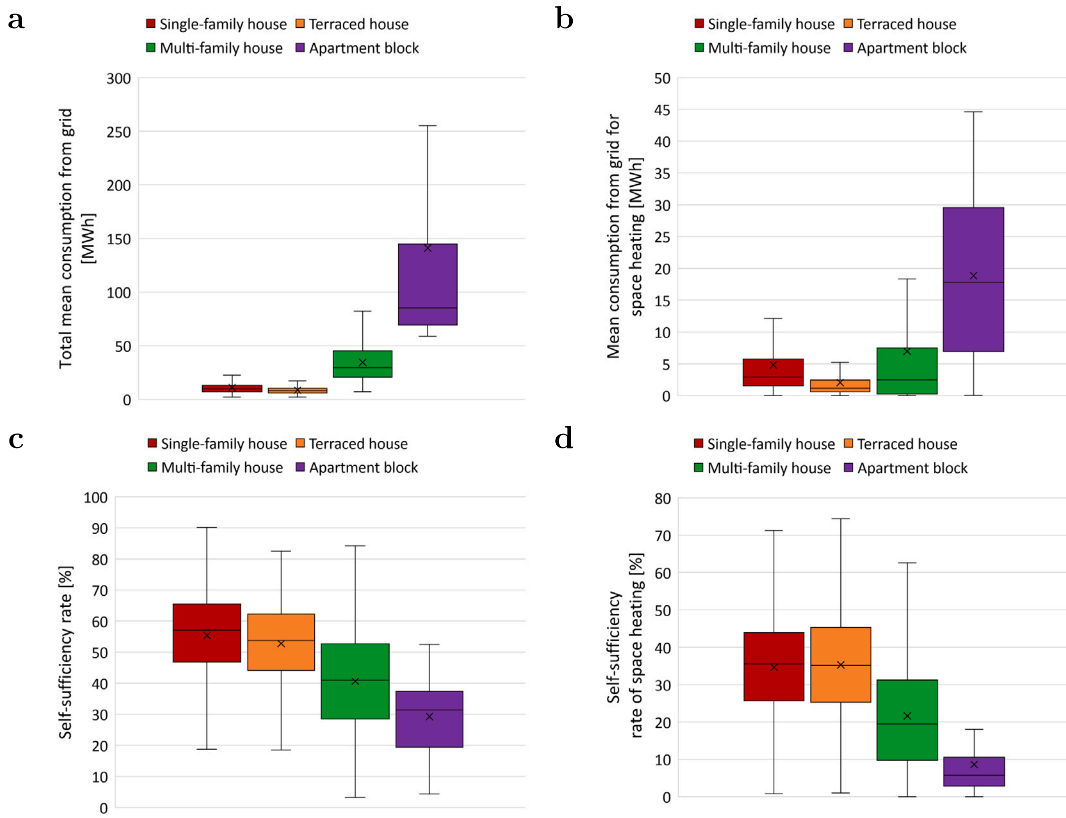

Fig. 3.3. Annual mean electricity consumption [MWh] and self-sufficiency rate [%] per building for the total building and for space heating only. The data is sorted according to building type. Outliers were removed. The *x* represents the mean value. (a) Total mean electricity consumption from grid per building [MWh] when no rooftop PV is used. (b) Mean electricity consumption from grid per building [MWh] for space heating when no rooftop PV is used. (c) Total self-sufficiency rate [%] per building. (d) Self-sufficiency rate of space heating [%] per building.

Statistics of residential energy consumption in Europe attribute 64.4% to space heating [1]. It must be noted that these values are based on the current state in all of Europe, where mostly fossil-fuel-based heating systems are used and many buildings remain unrefurbished (in Germany, only 5.1% of the building stock has been ambitiously renovated according to the Federal Environmental Agency [72]). In our study, we use heat pumps and floor heating systems, and the energy efficiencies in our German building dataset are higher than those reported by the Federal Environmental Agency [29], which might explain these differences. Due to the deviations in the shares of refurbishment states between ETHOS.BUILDA and the Federal Environmental Agency, the effect of energy efficiency on grid consumption and heat demand is not discussed in this paper. We estimate that the energy efficiencies of the buildings impact consumption, as shown in other studies [4,18,73], and well-insulated buildings reduce heat demand even further. For the future, it would be interesting to investigate the effect of the current German refurbishment states and to quantify the self-covered space heating demands if the entire building stock were fully renovated.

Regarding the weather profiles, we only considered TRY profiles from 2015. It would be of great interest to run the same analysis with future weather data to observe how residential heat, and especially cooling, demand develops in terms of climate change.

All our results are based on the energy system and building simulation model presented here, and all data are only an approximation of reality within certain constraints. Residential energy demand depends highly on the system's installation and control [14]. Our heat pump model from hplib [49] is generic and represents only an average of real heat pump efficiency parameters whereas in real systems heat pumps have different manufacturers and installations. In our rooftop PV system model from pvlib [55] we use PV modules and inverters from 2013 taken from the sandia database which are slightly less efficient than real PV modules and inverters currently on the market. The thermal properties of the buildings used in this study are based on the respective Tabula type. These are average values and might differ from real, individual building properties. Also the accuracy of the Tabula type assignment has limitations as discussed in Section 2.1.1. While building interactions and microclimate effects, such as urban heat islands and shading from surrounding buildings as described in Zhao et al. [74], play role for urban residential energy consumption, they are outside the scope of this study. These mechanisms are influenced by various factors, including climate, building density, height, layout, energy efficiency, user behavior, natural environment, and wind flow. Further research is needed to develop a deeper understanding of these impacts on German residential energy consumption. In general, all values are fitted and aggregated and no real values (occupancy, heating system efficiency, Tabula related building properties, weather profiles etc.) are used. We need to approximate data because real data is not available or limited. In the future more open-source data is needed to constantly improve the accuracy of energy system models.

The advantage of our method is that we can mimic dynamic and flexible processes and interactions between the individual energy system components with a high level of detail. One downside, compared to cost optimization models, is that our approach does not focus on the most economically beneficial energy system sizing and configurations, which might lead to different results compared to optimization-based studies [75]. To address this, for the next study, we would like to include a cost analysis and optimize our energy system configuration and control with respect to the least costs.

Overall, our model is capable of providing a detailed and large-scale bottom-up analysis of load profiles for building datasets and, therefore, can help understand the diverse interactions between occupants, building envelope, heating system, weather, PV production,

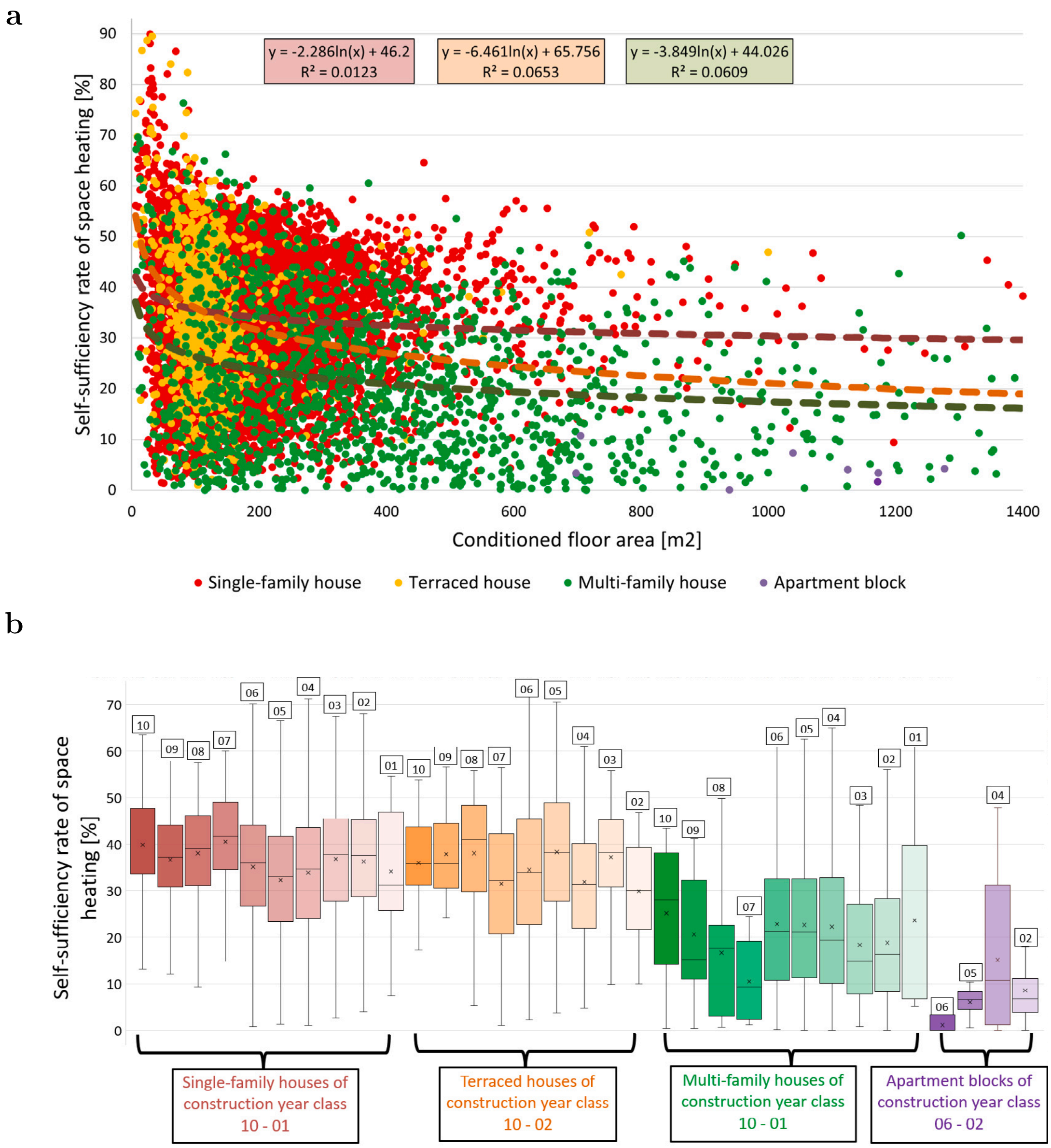

Fig. 3.4. Self-sufficiency rate [%] of space heating in our building dataset. (a) Self-sufficiency rate of space heating [%] sorted for different building types as a function of the conditioned floor area [m^2]. (b) Self-sufficiency rate [%] of space heating (SH) heat pump sorted according to building type and construction year class.

and energy management for a variety of buildings. The information gained from our simulations is crucial for stakeholders in the residential building and grid sectors and can support decision-making in the decarbonization process of the German building stock [15].

5. Conclusion and outlook

This paper explores how much of the annual residential heat demand in German households could be covered on-site using air–water heat pump systems combined with rooftop PV, energy management, and thermal and electric storage. We recreated the German building stock by selecting random residential buildings from the ETHOS. BUILDA database [26] and assigned each building random households, rooftop PV, and weather profiles. For each building, we ran dynamic energy load profile simulations with ETHOS.HiSim [24]. The energy systems were scaled based on normative heating load, building size, and number of dwellings. We evaluated a scenario where all electricity demand was provided from the grid versus a scenario where each building utilized its full rooftop PV potential.

We found that exploiting the full PV potential, together with energy management and thermal and electric storage, could reduce the electricity demand for space heating of the overall German building stock by 35.2%. The saving potential is particularly high for single-family and terraced houses (space heating self-sufficiency rate: SFH: 34.6%, TH: 35.3%, MFH: 21.6%, AB: 8.6%). The self-sufficiency rate for space heating decreases with increasing floor areas, with the decline being most significant for small areas but becoming more gradual for larger areas. In cold periods (October to March), SFH and TH buildings show mean grid consumptions that are 52%–70% lower than the average grid consumption without PV. In warm periods (April to September), THs and SFHs inject electricity into the grid with up to 90 kWh per day. This underscores the necessity of grid expansion in most regions of Germany.

Our method allowed for a large-scale, statistically based bottom-up analysis of building stock energy load profiles and dynamic building simulations of solar-assisted heat pump systems, which is of a larger scale than other studies found in the literature. The information on the heat demand that could be covered independently of the grid and the influencing factors can be valuable for stakeholders in the

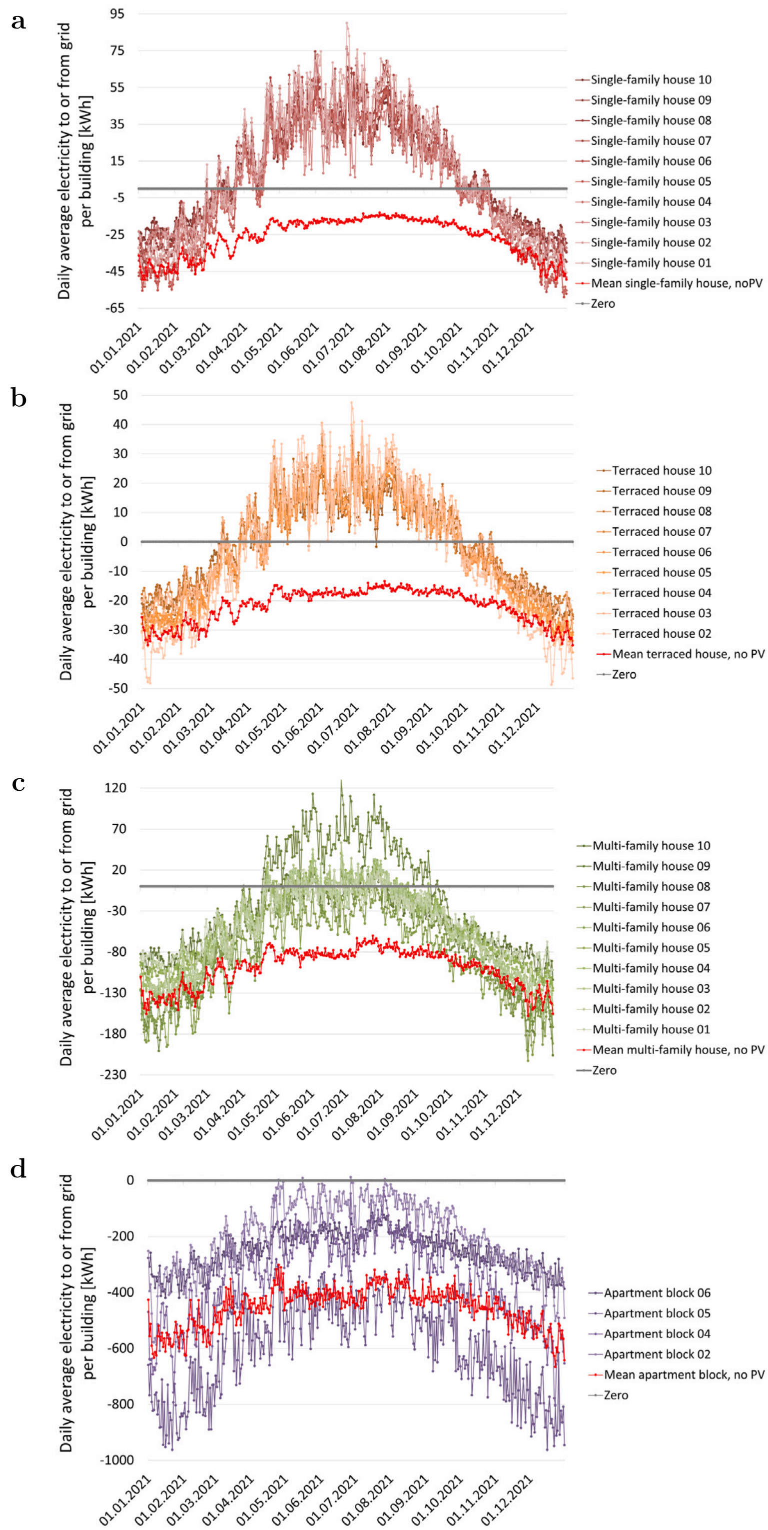

Fig. 3.5. Daily mean electricity to or from grid for different building types sorted according to their construction year classes 01–10 (explanation see Fig. A.1). (a) Daily electricity to or from grid for single-family houses (SFH). (b) Daily electricity to or from grid for terraced houses (TH). (c) Daily electricity to or from grid for multi-family houses (MFH). (d) Daily electricity to or from grid for apartment blocks (AB).

Table A.1
Average values of our building dataset for the case when full rooftop PV potential is used in combination with battery storage and energy management system. The total mean consumption is slightly higher as mentioned in Section 3 because of the battery losses and the demand-side management which increases consumption during periods of excess supply.

Parameter	Mean value	Unit
Conditioned floor area	239	m^2
Norm heating load	11	kW
Number of dwellings	2.2	–
Number of residents per dwelling	2.1	–
Rooftop area	191	m^2
PV azimuth angle	183	°
PV tilt angle	32	°
PV rooftop capacity	15.5	kW
PV rooftop generation	13.5	MWh
Total electricity consumption	15.5	MWh
Consumption from grid	8.5	MWh
Injection to grid	6.2	MWh

Statistic S-1.1: Frequency of building types of the national building stock

(building stock in May 2011: residential buildings erected until end of 2009)
total residential building stock in May 2011: 18,368,000 buildings, 39,432,000 apartments, 3,575 million m² living space

construction		SFH	TH	MFH	AB	sum	fraction
year class		number of buildings (1000)					
1	... 1859	330	148	54	0.6	533	3 %
2	1860 ... 1918	966	492	442	28.7	1929	11 %
3	1919 ... 1948	1131	710	388	7.4	2236	12 %
4	1949 ... 1957	859	447	356	17.3	1679	9 %
5	1958 ... 1968	1509	633	586	34.0	2762	15 %
6	1969 ... 1978	1507	611	412	50.1	2580	14 %
7	1979 ... 1983	704	335	146	15.0	1200	7 %
8	1984 ... 1994	1160	652	309	28.7	2150	12 %
9	1995 ... 2001	1035	619	244	20.9	1919	11 %
10	2002 ... 2009	775	384	85	7.6	1251	7 %
sum		9976	5030	3023	210	18239	100 %
fraction		55 %	28 %	17 %	1 %	100 %	

Last updated: 31.10.2013

Fig. A.1. Tabula statistic on the building codes of the German building stock in 2011 [36,37].

Table A.2
Weather stations and regions of Test-Reference Years (TRY) data [76].

No.	Lon.	Lat.	Temp. [°C]	Station	Region
1	53.5591	8.5872	10.0	Bremerhaven	North Sea coast
2	54.0878	12.1088	9.8	Rostock	Baltic Sea coast
3	53.5299	10.0078	9.7	Hamburg	Northwest German Lowland
4	52.3938	13.0651	9.9	Potsdam	Northeast German Lowland
5	51.4562	7.0568	10.9	Essen	Lower Rhine-Westphalian Bay and Emsland
6	50.6461	7.9426	8.5	Bad Marienburg	Northern and western uplands, peripheral areas
7	51.3334	9.4725	9.8	Kassel	Northern/western uplands, central areas
8	51.7239	10.6069	6.7	Braunlage	Upper Harz and Black Forest (middle elevations)
9	50.8233	12.9181	9.5	Chemnitz	Thuringian Basin and Saxon Upland
10	50.3226	11.9124	8.3	Hof	Southeastern uplands up to 1000 m
11	50.4312	12.9522	4.0	Fichtelberg	Erzgebirge, Bohemian and Black Forest over 1000 m
12	49.4902	8.4637	12.1	Mannheim	Upper Rhine Valley and lower Neckar Valley
13	48.2432	12.5286	8.8	Mühldorf	Swabian-Franconian Upland/Alpine Foreland
14	48.6536	9.8666	8.0	Stötten	Swabian Alb/Baar
15	47.4945	11.1046	7.6	Garmisch-Partenkirchen	Alpine foothills/valleys

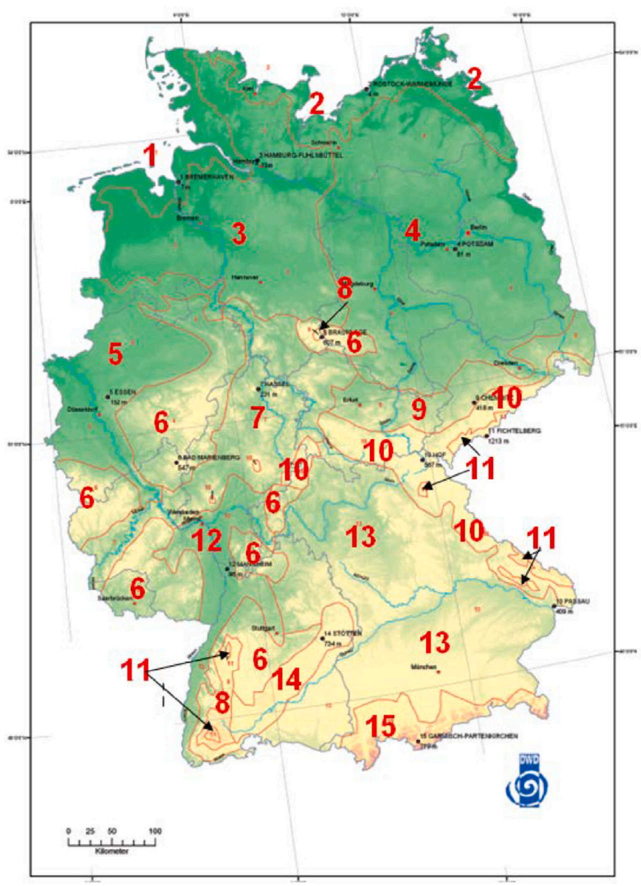

Fig. A.2. Test Reference Years (TRY) regions distributed over Germany [76,77].

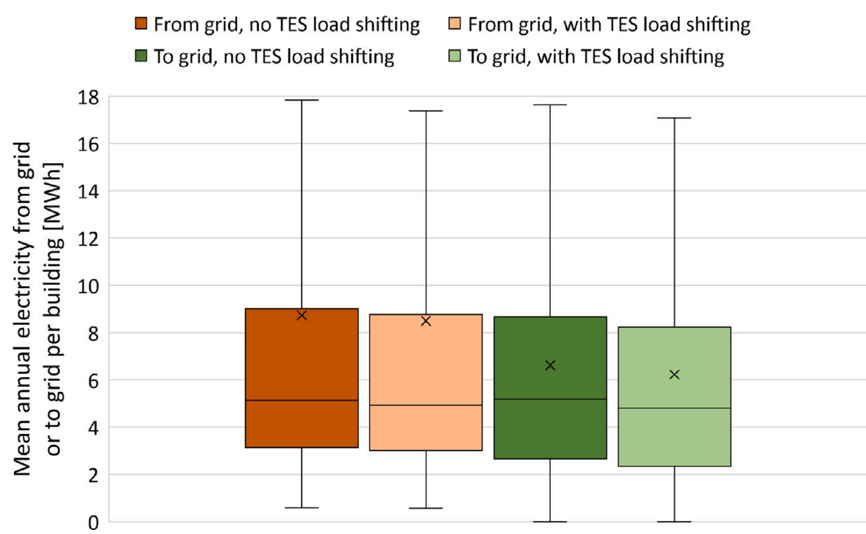

Fig. A.3. Mean annual electricity from grid (orange) and to grid (green) per building [MWh] for residential energy systems with and without thermal energy storage (TES) load shifting.

residential building and grid sectors and can support decision-making in the decarbonization process of the German building stock.

CRediT authorship contribution statement

Katharina Rieck: Writing – review & editing, Writing – original draft, Visualization, Validation, Software, Methodology, Investigation, Formal analysis, Data curation, Conceptualization. **Kristina Dabrock:** Writing – original draft, Methodology, Conceptualization. **Noah Pflugradt:** Supervision, Resources, Project administration, Funding acquisition, Conceptualization. **Jann Michael Weinand:** Writing – review & editing. **Detlef Stolten:** Resources.

Declaration of Generative AI and AI-assisted technologies in the writing process

During the preparation of this work the authors used "ChatGPT" by OpenAI in order to check grammar and spelling in a few places, and to make minor improvements to readability and style. After using this tool, the authors reviewed and edited the content as needed and take full responsibility for the content of the published article.

Declaration of competing interest

The authors declare that they have no known competing financial interests or personal relationships that could have appeared to influence the work reported in this paper.

Acknowledgments

The authors would like to express their gratitude to the Federal Ministry for Economic Affairs and Climate Action (BMWK.IIB4) for providing the necessary resources to conduct this study. Our research was supported by the WAAGE Grant Program (Grant No. 03EI1044/03EE 5031D), and we appreciate their financial assistance.

Appendix

See Tables A.1 and A.2, Figs. A.1–A.3.

Data availability

Data will be made available on request.

References

[1] eurostat Statistics Explained. Energy consumption in households. 2023, URL https://ec.europa.eu/eurostat/statisticsexplained/.

[2] Agency EE, Commission E, Action DC. Annual European Union greenhouse gas inventory 1990–2021 and inventory report 2023. 2023, URL https://www.eea.europa.eu/publications/annual-european-union-greenhouse-gas-2.

[3] Agency EE. Greenhouse gas emissions from energy use in buildings in Europe. 2023, URL https://www.eea.europa.eu/en/analysis/indicators/greenhouse-gas-emissions-from-energy.

[4] Bee E, Prada A, Baggio P, Psimopoulo E. Air-source heat pump and photovoltaic systems for residential heating and cooling: Potential of self-consumption in different European climates. Build Simul 2019;12:453–63, URL https://link.springer.com/article/10.1007/s12273-018-0501-5.

[5] Wang C, Gong G, Su H, Wah Yu C. Efficacy of integrated photovoltaics-air source heat pump systems for application in Central-south China. Renew Sustain Energy Rev 2015;49:1190–7. http://dx.doi.org/10.1016/j.rser.2015.04.172, URL https://linkinghub.elsevier.com/retrieve/pii/S1364032115004426.

[6] Wang Z, Luther MB, Horan P, Matthews J, Liu C. On-site solar PV generation and use: Self-consumption and self-sufficiency. Build Simul 2023. http://dx.doi.org/10.1007/s12273-023-1007-3, URL https://link.springer.com/10.1007/s12273-023-1007-3.

[7] Aneli S, Arena R, Marco Tina G, Gagliano A. Improvement of energy self-sufficiency in residential buildings by using solar-assisted heat pumps and thermal and electrical storage. Sustain Energy Technol Assess 2023;60:103446. http://dx.doi.org/10.1016/j.seta.2023.103446, URL https://linkinghub.elsevier.com/retrieve/pii/S2213138823004393.

[8] Battaglia M, Haberl R, Bamberger E, Haller M. Increased self-consumption and grid flexibility of PV and heat pump systems with thermal and electrical storage. Energy Procedia 2017;135:358–66. http://dx.doi.org/10.1016/j.egypro.2017.09.527, URL https://linkinghub.elsevier.com/retrieve/pii/S1876610217346398.

[9] Zhang X, Xiao F, Li Y, Ran Y, Gao W. Flexible coupling and grid-responsive scheduling assessments of distributed energy resources within existing zero energy houses. J Build Eng 2024;87:109047. http://dx.doi.org/10.1016/j.jobe.2024.109047, URL https://linkinghub.elsevier.com/retrieve/pii/S2352710224006156.

[10] Yu S, Liu X, Li R, Yin Z, Chen Z, Han F, Li S. Demand side management full season optimal operation potential analysis for coupled hybrid photovoltaic/thermal, heat pump, and thermal energy storage systems. J Energy Storage 2024;80:110375. http://dx.doi.org/10.1016/j.est.2023.110375, URL https://linkinghub.elsevier.com/retrieve/pii/S2352152X2303774X.

[11] Perrella S, Bisegna F, Bevilacqua P, Cirone D, Bruno R. Solar-assisted heat pump with electric and thermal storage: The role of appropriate control strategies for the exploitation of the solar source. Buildings 2024;14(1):296. http://dx.doi.org/10.3390/buildings14010296, URL https://www.mdpi.com/2075-5309/14/1/296.

[12] Bae S, Chae H, Nam Y. Experimental analysis of an integrated system using photovoltaic–thermal and air source heat pump for real applications. Renew Energy 2023;217:119128. http://dx.doi.org/10.1016/j.renene.2023.119128, URL https://linkinghub.elsevier.com/retrieve/pii/S096014812301042X.

[13] Tagliafico LA, Arteconi A, Cavalletti A, Marafioti C, Marchitto A. Performance of a solar assisted heat pump for building heating: Control problems and improvements. J Phys Conf Ser 2020;1599(1):012036. http://dx.doi.org/10.1088/1742-6596/1599/1/012036, URL https://iopscience.iop.org/article/10.1088/1742-6596/1599/1/012036.

[14] Franco A, Fantozzi F. Experimental analysis of a self consumption strategy for residential building: The integration of PV system and geothermal heat pump. Renew Energy 2016;86:1075–85. http://dx.doi.org/10.1016/j.renene.2015.09.030, URL https://linkinghub.elsevier.com/retrieve/pii/S0960148115303098.

[15] Wärmepumpen im Gebäudesektor - Eine technologie für eine fossilfreie wärmeversorgung. Tech. rep., Deutsche Energie-Agentur GmbH (dena); 2023, URL https://www.dena.de/infocenter/waermepumpen-im-gebaeudesektor/.

[16] Commission E. Communication from the commission to the European parliament, the Council, the European economic and social Committee and the Committee of the Regions - EU solar energy strategy. 2022, URL https://eur-lex.europa.eu/legal-content/EN/TXT/?uri=COM%3A2022%3A221%3AFIN&qid=1653034500503.

[17] Protopapadaki C, Saelens D. Heat pump and PV impact on residential low-voltage distribution grids as a function of building and district properties. Appl Energy 2017;192:268–81. http://dx.doi.org/10.1016/j.apenergy.2016.11.103, URL https://linkinghub.elsevier.com/retrieve/pii/S0306261916317329.

[18] Arens S, Schluters S, Hanke B, Von Maydell K, Agert C. Monte-Carlo evaluation of residential energy system morphologies applying device agnostic energy management. IEEE Access 2022;10:7460–75. http://dx.doi.org/10.1109/ACCESS.2021.3138549, URL https://ieeexplore.ieee.org/document/9663153/.

[19] Kleinebrahm M, Weinand JM, Naber E, McKenna R, Ardone A. Analysing municipal energy system transformations in line with national greenhouse gas reduction strategies. Appl Energy 2023;332:120515. http://dx.doi.org/10.1016/j.apenergy.2022.120515, URL https://linkinghub.elsevier.com/retrieve/pii/S030626192201772X.

[20] Kleinebrahm M, Weinand JM, Naber E, McKenna R, Ardone A, Fichtner W. Two million European single-family homes could abandon the grid by 2050. Joule 2023;7(11):2485–510. http://dx.doi.org/10.1016/j.joule.2023.09.012, URL https://linkinghub.elsevier.com/retrieve/pii/S2542435123004026.

[21] Fraga C, Hollmuller P, Schneider S, Lachal B. Heat pump systems for multifamily buildings: Potential and constraints of several heat sources for diverse building demands. Appl Energy 2018;225:1033–53. http://dx.doi.org/10.1016/j.apenergy.2018.05.004, URL https://linkinghub.elsevier.com/retrieve/pii/S0306261918306974.

[22] Mascherbauer P, Kranzl L, Yu S, Haupt T. Investigating the impact of smart energy management system on the residential electricity consumption in Austria. Energy 2022;249:123665. http://dx.doi.org/10.1016/j.energy.2022.123665, URL https://linkinghub.elsevier.com/retrieve/pii/S0360544222005680.

[23] Wagner A, Ruellan M, Heinrich M, Bourdais R. Towards a classification of the building stock in terms of potential energy savings through advanced control. Energy Build 2024;310:114050. http://dx.doi.org/10.1016/j.enbuild.2024.114050, URL https://linkinghub.elsevier.com/retrieve/pii/S037877882400166X.

[24] Pflugradt N. ETHOS.HiSim - House infrastructure simulator. MIT, URL https://github.com/FZJ-IEK3-VSA/HiSim.

[25] Scholle K. Anzahl der Wohngebäude in Deutschland in den Jahren von 1995 bis 2022. 2024, URL https://de.statista.com/statistik/daten/studie/70094/umfrage/wohngebaeude-bestand-in-deutschland-seit-1994/#:~:text=Wohngeb%C3%A4ude%20%2D%20Bestand%20in%20Deutschland%20bis%202022&text=Im%20Jahr%202022%20wurden%20in,19%2C5%20Millionen%20Wohngeb%C3%A4ude%20gez%C3%A4hlt.

[26] Dabrock K, Ulken J, Pflugradt N, Weinand J, Stolten D. ETHOS.BUILDA: Residential building TABULA archetype dataset Germany. 2024, URL https://zenodo.org/records/12069755.

[27] Risch S, Maier R, Du J, Pflugradt N, Stenzel P, Kotzur L, Stolten D. Potentials of renewable energy sources in Germany and the influence of land use datasets. Energies 2022;15(15):5536. http://dx.doi.org/10.3390/en15155536, URL https://www.mdpi.com/1996-1073/15/15/5536.

[28] Zensus 2011: Zensus kompakt – endgültige ergebnisse. 2014, URL www.statistik-bw.de.

[29] Dabrock K, Ulken J, Pflugradt N, Weinand JM, Stolten D. Generating a nationwide residential building types dataset using machine learning. 2024, http://dx.doi.org/10.2139/ssrn.4884155.

[30] Loga T, Stein B, Diefenbach N. TABULA building typologies in 20 European countries—Making energy-related features of residential building stocks comparable. Energy Build 2016;132:4–12. http://dx.doi.org/10.1016/j.enbuild.2016.06.094, URL https://linkinghub.elsevier.com/retrieve/pii/S0378778816305837.

[31] Dascalaki EG, Droutsa KG, Balaras CA, Kontoyiannidis S. Building typologies as a tool for assessing the energy performance of residential buildings – A case study for the Hellenic building stock. Energy Build 2011;43(12):3400–9. http://dx.doi.org/10.1016/j.enbuild.2011.09.002, URL https://linkinghub.elsevier.com/retrieve/pii/S0378778811003902.

[32] Vimmr T, Loga T, Diefenbach N, Stein B, Bachová L. TABULA – Residential building typologies in 12 European Countries – Good practice example from the Czech Republic. 2013, URL https://www.cesb.cz/cesb13/proceedings/5_tools/CESB13_1200.pdf.

[33] Ignjatović D, Bojana Z, Ćuković Ignjatović N, Đukanović L, Radivojević A, Rajčić A. Methodology for residential building stock refurbishment planning—Development of local building typologies. Sustainability 2021;13(8):4262. http://dx.doi.org/10.3390/su13084262, URL https://www.mdpi.com/2071-1050/13/8/4262.

[34] Ballarini I, Corgnati SP, Corrado V. Use of reference buildings to assess the energy saving potentials of the residential building stock: The experience of TABULA project. Energy Policy 2014;68:273–84. http://dx.doi.org/10.1016/j.enpol.2014.01.027, URL https://linkinghub.elsevier.com/retrieve/pii/S0301421514000329.

[35] Hettinga S, Van 'T Veer R, Boter J. Large scale energy labelling with models: The EU TABULA model versus machine learning with open data. Energy 2023;264:126175. http://dx.doi.org/10.1016/j.energy.2022.126175, URL https://linkinghub.elsevier.com/retrieve/pii/S0360544222030614.

[36] Diefenbach N. Basisdaten für hochrechnungen mit der deutschen gebäudetypologie des IWU: Neufassung oktober 2013. 2013, URL https://www.iwu.de/fileadmin/publikationen/energie/klima_altbau/2013_IWU_Diefenbach_Basisdaten-f¨ur-Hochrechnungen-mit-der-Deutschen-Geb¨audetypologie-des-IWU-2013.pdf.

[37] Episcope. Statistics of the german building stock. 2014, URL https://episcope.eu/building-typology/country/de.html.

[38] für Solare Energiesysteme ISE F-I. Wärmepumpen in bestandsgebäuden - ergebnisse aus dem forschungsprojekt "wpsmart im bestand" - abschlussbericht. 2020, URL https://www.ise.fraunhofer.de/content/dam/ise/de/downloads/pdf/Forschungsprojekte/BMWi-03ET1272A-WPsmart_im_Bestand-Schlussbericht.pdf.

[39] Bai X. Analysis of the advantages and disadvantages of BIPV technology. Appl Comput Eng 2023;9(1):204–9. http://dx.doi.org/10.54254/2755-2721/9/20230090, URL https://www.ewadirect.com/proceedings/ace/article/view/4213.

[40] greenbuddieseu. Photovoltaic facade systems - a way to integrate green energy into the building structure. 2023, URL https://www.greenbuddies.eu/en/blog/photovoltaic-facade-systems-a-way-to-integrate-green-energy-into-the-building-structure.

[41] Valerius G. Photovoltaik an der Fassade montieren. 2024, URL https://www.solaranlage-ratgeber.de/photovoltaik/photovoltaik-installation/photovoltaik-an-der-fassade#google_vignette.

[42] Orhon AV. A review on adaptive photovoltaic facades. In: Solar conference & exhibition solar TR2016. 2016, URL https://www.researchgate.net/publication/327776050_A_Review_on_Adaptive_Photovoltaic_Facades/figures?lo=1.

[43] Ryberg DS. Generation lulls from the future potential of wind and solar energy in Europe. Schriften des forschungszentrums jülich - energie & umwelt / energy & environment, Vol. 521, 2020, URL https://publications.rwth-aachen.de/record/805445.

[44] Killinger S, Lingfors D, Saint-Drenan Y-M, Moraitis P, Van Sark W, Taylor J, Engerer NA, Bright JM. On the search for representative characteristics of PV systems: Data collection and analysis of PV system azimuth, tilt, capacity, yield and shading. Sol Energy 2018;173:1087–106. http://dx.doi.org/10.1016/j.solener.2018.08.051, URL https://linkinghub.elsevier.com/retrieve/pii/S0038092X18308211.

[45] Schwochow M. Postleitzahlen Deutschland. 2024, URL https://www.suche-postleitzahl.org/downloads.

[46] Institut für Normung e. V. DD, Heiz-und Raumlufttechnik sowie deren Sicherheit (NHRS) D-N. Method for calculation of the room heat load - part 1: National addition to DIN EN 12831-1, with CD-ROM. 2020, URL https://www.dinmedia.de/de/vornorm/din-ts-12831-1/316645651.

[47] Vámos V, Horváth M. The effect of building refurbishment and changing occupancy on the district heating consumption of multifamily buildings: Case study of Miskolc, Hungary. J Build Eng 2024;81:108132. http://dx.doi.org/10.1016/j.jobe.2023.108132, URL https://linkinghub.elsevier.com/retrieve/pii/S2352710223023124.

[48] Pflugradt N, Stenzel P, Kotzur L, Stolten D. LoadProfileGenerator: An agent-based BehaviorSimulation for generating residential load profiles. J Open Source Softw 2022;7(71):3574. http://dx.doi.org/10.21105/joss.03574, URL https://joss.theoj.org/papers/10.21105/joss.03574.

[49] Hoops H, Tjaden T, Rösken K. RE-Lab-projects/hplib: v1.9. 2022, URL https://github.com/FZJ-IEK3-VSA/hplib.

[50] Schwamberger K. Modellbildung und regelung von gebäudeheizungsanlagen mit wärmepumpen. 1991, URL https://katalog.slub-dresden.de/id/0-27191484X.

[51] Jülich SI. CARNOT - Conventional and renewable energy systems optimization toolbox - version 5.3. 2012, URL https://de.mathworks.com/matlabcentral/fileexchange/68890-carnot-toolbox.

[52] Tjaden T, Schnorr F, Weniger J, Bergner J, Quaschning V. Einsatz von PV-systemen mit wärmepumpen und batteriespeichern zur erhöhung des autarkiegrades in einfamilienhaushalten. 2015, http://dx.doi.org/10.13140/RG.2.1.4033.9044, URL http://rgdoi.net/10.13140/RG.2.1.4033.9044, Publisher: Unpublished.

[53] Olesen BW. Radiant floor heating in theory and practice. ASHRAE J 2002;44(7). URL https://www.researchgate.net/publication/279557548_Radiant_floor_heating_in_theory_and_practice.

[54] O'Hegarty R, Kinnane O, Lennon D, Colclough S. Air-to-water heat pumps: Review and analysis of the performance gap between in-use and product rated performance. Renew Sustain Energy Rev 2022;155:111887. http://dx.doi.org/10.1016/j.rser.2021.111887, URL https://linkinghub.elsevier.com/retrieve/pii/S1364032121011540.

[55] F. Holmgren W, W. Hansen C, A. Mikofski M. Pvlib python: a python package for modeling solar energy systems. J Open Source Softw 2018;3(29):884. http://dx.doi.org/10.21105/joss.00884, URL http://joss.theoj.org/papers/10.21105/joss.00884.

[56] Holmgren WF, Groenendyk DG. An open source solar power forecasting tool using PVLIB-Python. In: 2016 IEEE 43rd photovoltaic specialists conference (PVSC). Portland, OR, USA: IEEE; 2016, p. 0972–5. http://dx.doi.org/10.1109/PVSC.2016.7749755, URL http://ieeexplore.ieee.org/document/7749755/.

[57] Andrews RW, Stein JS, Hansen C, Riley D. Introduction to the open source PV LIB for python Photovoltaic system modelling package. In: 2014 IEEE 40th photovoltaic specialist conference (PVSC). Denver, CO, USA: IEEE; 2014, p. 0170–4. http://dx.doi.org/10.1109/PVSC.2014.6925501, URL http://ieeexplore.ieee.org/document/6925501/.

[58] Rösken K, Tjaden T, Hoops H. RE-lab-projects/bslib: v0.1. 2022, URL https://github.com/FZJ-IEK3-VSA/bslib.

[59] Jayathissa P, Luzzatto M, Schmidli J, Hofer J, Nagy Z, Schlueter A. Optimising building net energy demand with dynamic BIPV shading. Appl Energy 2017;202:726–35. http://dx.doi.org/10.1016/j.apenergy.2017.05.083, URL https://linkinghub.elsevier.com/retrieve/pii/S0306261917305810.

[60] ISO. Energy performance of buildings. Calculation of energy use for space heating and cooling. 2007, http://dx.doi.org/10.3403/30133624, URL https://linkresolver.bsigroup.com/junction/resolve/000000000030133624?restype=standard.

[61] Team TP. Typology approach for building stock energy assessment. main results of the TABULA project. 2012, URL www.building-typology.eu.

[62] Baunetz_Wissen_. Dimensionierung von Pufferspeichern. 2024, URL https://www.baunetzwissen.de/heizung/fachwissen/speicher/dimensionierung-von-pufferspeichern-161296.

[63] Weniger J, Tjaden T, Quaschning V. Sizing of residential PV battery systems. Energy Procedia 2014;46:78–87. http://dx.doi.org/10.1016/j.egypro.2014.01.160, URL https://linkinghub.elsevier.com/retrieve/pii/S1876610214001763.

[64] Energie-Agentur D. Dena-gebäudereport 2024 - zahlen, daten, fakten zum klimaschutz im gebäudebestand. 2023, URL www.gebaeudeforum.de/gebaeudereport2024.

[65] Lentner F, Walter W, Stiewe C. Short-term forecasting of gas consumption by standard load profiles in Germany. Ger Econ Team 2021. URL https://www.german-economic-team.com/wp-content/uploads/2022/02/GET_UZB_TN_07_2021_en.pdf.

[66] Mirkov R, Friedl H, Leovey H, Wegner-Specht I. Sigmoid models utilized in optimization of gas transportation networks. 2010, URL https://www.researchgate.net/publication/267408526_Sigmoid_Models_Utilized_in_Optimization_of_Gas_Transportation_Networks.

[67] Leövey H, Römisch W, Wegner-Specht I, Steinkamp A. Modellierung der gasabnahme als funktion der temperatur: Optimierung der temperaturgewichte. 2011, URL https://www2.mathematik.hu-berlin.de/~romisch/papers/LRSW11gwf.pdf.

[68] Ravnik J, Jovanovac J, Trupej A, Vištica N, Hriberšek M. A sigmoid regression and artificial neural network models for day-ahead natural gas usage forecasting. Clean Responsib Consum 2021;3:100040. http://dx.doi.org/10.1016/j.clrc.2021.100040, URL https://linkinghub.elsevier.com/retrieve/pii/S2666784321000346.

[69] Eicke A, Hirth L, Mühlenpfordt J. Mehrwert dezentraler Flexibilität. Elektro- und Digitalindustrie (ZVEI e.V.); 2024, URL https://neon.energy/mehrwert-flex/.

[70] Bundesamt S. Stromverbrauch der privaten haushalte nach haushaltsgrößenklassen. 2023, URL https://www.destatis.de/DE/Themen/Gesellschaft-Umwelt/Umwelt/UGR/private-haushalte/Tabellen/stromverbrauch-haushalte.html.

[71] Burger B, Energy-Charts. Nettostromerzeugung in deutschland im Jahr 2023. 2024, URL https://www.energy-charts.info/index.html?l=de&c=DE.

[72] Umweltbundesamt. Wohnen und sanieren - empirische wohngebäudedaten seit 2002. Co2online Gemeinnützige GmbH; 2019, URL http://www.umweltbundesamt.de/publikationen.

[73] Knuutila M, Kosonen A, Jaatinen-Värri A, Laaksonen P. Profitability comparison of active and passive energy efficiency improvements in public buildings. Energy Effic 2022;15(6):38. http://dx.doi.org/10.1007/s12053-022-10046-9, URL https://link.springer.com/10.1007/s12053-022-10046-9.

[74] Zhao Y, Ding X, Wu Z, Yin S, Fan Y, Ge J. Impact of urban form on building energy consumption in different climate zones of China. Energy Build 2024;320:114579. http://dx.doi.org/10.1016/j.enbuild.2024.114579, URL https://linkinghub.elsevier.com/retrieve/pii/S0378778824006959.

[75] Weinand JM, Hoffmann M, Göpfert J, Terlouw T, Schönau J, Kuckertz P, McKenna R, Kotzur L, Linßen J, Stolten D. Global LCOEs of decentralized off-grid renewable energy systems. Renew Sustain Energy Rev 2023;183:113478. http://dx.doi.org/10.1016/j.rser.2023.113478, URL https://linkinghub.elsevier.com/retrieve/pii/S1364032123003350.

[76] (DWD) DW, Bundesamt für Bauwesen und Raumordnung (BBR). Handbuch - ortsgenaue testreferenzjahre von deutschland für mittlere, extreme und zukünftige Witterungsverhältnisse. 2017, URL https://www.bbsr.bund.de/BBSR/DE/forschung/programme/zb/Auftragsforschung/5EnergieKlimaBauen/2013/testreferenzjahre/try-handbuch.pdf?_blob=publicationFile&v=6.

[77] ubakus. TRY-regionen deutschlands. 2024, URL https://www.ubakus.de/try-regionen-deutschlands/.